

Predominance of Prolate Nuclear Deformations Emerging from Many-Body Interactions

Mihai Horoi

Department of Physics, Central Michigan University, Mount Pleasant, Michigan 48859, USA

Vladimir Zelevinsky

*National Superconducting Cyclotron Laboratory, East Lansing,
Michigan 48824, USA, and Department of Physics and Astronomy,
Michigan State University, East Lansing, Michigan 48824, USA*

(Dated: September 5, 2021)

A new approach to the old problem of the predominance of prolate deformations among well deformed nuclei is proposed within the shell model framework. The parameter space is explored using the ensemble of random rotationally-invariant interactions. Subsets with rotational energy ratio $E(4^+)/E(2^+)$ and the rigid-rotor relation between the quadrupole moment $Q(2^+)$ and the transition probability $B(E2; 2^+ \rightarrow 0^+)$ are found exhibiting prolate predominance. We identify matrix elements of the effective forces responsible for the predominance of prolate deformation.

PACS numbers: 21.60.Cs, 21.10.Re, 21.60.Ka

The majority of deformed nuclei have axially symmetric prolate deformation in their ground state (g.s.). The presence of rotational bands with typical energy intervals is the first signature of stable deformation. The states in a band are connected by strong quadrupole transitions obeying simple rigid rotor intensity rules. The same rules [1] determine the expectation values of multipole operators. This is essentially a projection of nearly constant within the band intrinsic (body-fixed) quantities onto the laboratory (space-fixed) coordinate frame. The overwhelmingly positive sign of the intrinsic quadrupole moment manifests the dominance of prolate deformation. The Nilsson diagram shows a pattern of split spherical single-particle orbitals that seems to be more or less symmetric with respect to the sign of deformation; the difference in the liquid drop energy for the two signs of deformation is pretty small [2]. While the results of the numerous mean field calculations for specific nuclei in general correctly predict the presence and the sign of deformation, the underlying physical reason for the predominance of prolate shapes is unclear.

It was argued by Lemmer [3] that the kinetic energy should contain an additional contribution similar to the term $-D\ell^2$ introduced by Nilsson [4] for interpolation between the harmonic oscillator and potential box. Being split to time-conjugate pairs $(m, -m)$ by deformation, the large- ℓ spherical orbitals determine the single-particle (s.p.) occupancies in the way that makes the prolate case energetically favorable. Related arguments were given by Castel and Goeke [5], who showed that the collective inertial parameter is larger for the prolate deformation, and later by Castel, Rowe and Zamick [6] with the help of self-consistency conditions [1]. There are also ideas based on the semiclassical analysis of the s.p. level density [7], simplest periodic orbits [8] and their bifurcations in a deformed cavity [9]. The predomi-

nance of prolate deformation analogously emerges in s.p. motion in metallic clusters [10] and for many biological objects, from molecular level to pollen grains [11]. The latest analysis by Hamamoto and Mottelson [12] starting with the statement that “the nature of the parameters responsible for the prolate dominance has not yet been adequately understood” proceeds along similar lines. Detailed calculations and comparison between the harmonic oscillator potential and that of a spheroidal cavity show a different character of the mixing of spherical orbitals for the prolate and oblate cases. Being a surface effect, the difference should decrease in large systems. The authors of Ref. [12] mention additional factors which were not sufficiently accounted for including the role of the spin-orbit potential, pairing effects [13], and the presence of two kinds of particles.

Below we suggest a new approach to this problem that was previously attacked from the viewpoint of the deformed mean field and corresponding quasiparticle motion. As the mean field itself is generated by the nucleon-nucleon interactions, it makes sense to take a step back and consider the many-body problem rather than the resulting s.p. motion. This would allow us to avoid questions of self-consistency and take into account not only pairing and spin-orbit forces but the full inter-particle interaction. The natural framework is provided by the shell model (SM) with effective interactions; modern versions of the SM give good agreement with the data. The exact diagonalization of the Hamiltonian matrix, with all conservation laws strictly respected, provides the eigenstates in the space-fixed frame; the spectrum and observables can be analyzed similarly to the experimental data. The problem requires exploration of the parameter space of the SM Hamiltonians in a sufficiently large orbital space.

To explore the parameter space we will work with random interactions. All two-body matrix elements allowed

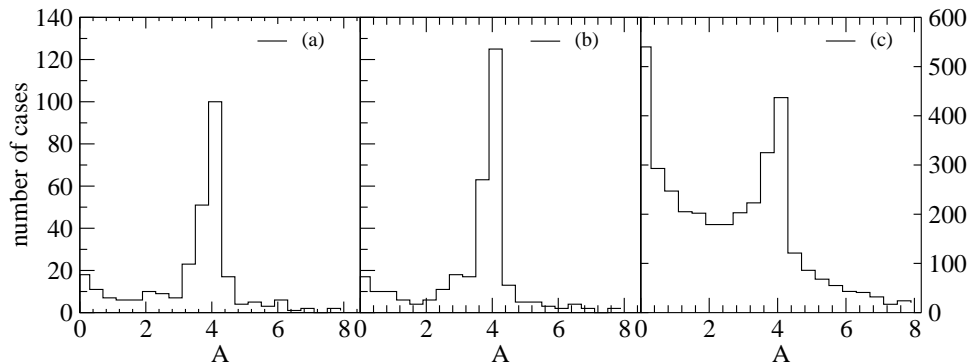


FIG. 1: The distribution of the Alaga ratio, Eq. (1), for all cases selected by the energy ratio $E(4)/E(2)$; the interaction strength is $\lambda = 0.5$, panel a, and $\lambda = 4$, panel b; the same for all cases with the sequence $(0^+, 2^+)$, panel c.

by angular momentum, parity and isospin conservation are taken as random uncorrelated quantities. Among many realizations of such an ensemble we can identify those with definite rotational characteristics and study the abundance of such cases and their dynamic origin. Random interactions in many-body systems are usually analyzed for studies of quantum chaos [14, 15] in relation to the random matrix theory. In Ref. [16] the ensemble was constructed with rotationally invariant interactions, and only the magnitudes of allowed matrix elements were taken randomly. The unexpected output was the discovery of the predominance, for an even number of particles, of the zero ground state spin, in spite of relatively low multiplicity of $J = 0$ states in Hilbert space. This result, valid not only in a single- j case but in the context of realistic SM space [17] as well, was fully understood in terms of geometry of the parameter space only for the exceptional case of the single $j = 7/2$ shell [18] and for the similar results in the interacting boson model [19]. In more realistic fermionic models the full theory is still absent; the most promising are the ideas of geometric chaoticity of random angular momentum coupling [20, 21]. The details were discussed in the review articles [22, 23, 24].

The rotationally invariant random interaction models provide a wealth of information. Any given set of random interaction parameters gives rise to a specific version of the SM. It was noticed, for example, that some sequences of the lowest excited states, like $0^+ - 2^+ - 4^+ - \dots$, appear with the enhanced probability. The energy ratios in such yrast sequences are spread around the values close to limiting cases of the collective models, such as vibrational and rotational bands [25]. In Ref. [22], the realizations with the lowest states $0^+ - 2^+$ were analyzed in terms of the Alaga ratio,

$$A = \frac{Q(2^+)^2}{B(E2; 2^+ \rightarrow 0^+)}, \quad (1)$$

of the squared expectation value of the quadrupole moment of the 2^+ state to the reduced transition probability from this state to the g.s. The distribution of the Alaga ratio reveals two pronounced peaks, close to zero and

	λ	$N(0, 2)$	$\frac{N(Q < 0)}{N(0, 2)}$	$N(E4/E2)$	N_{rot}	$\frac{N_{\text{prolate}}}{N_{\text{rot}}}$
(a)	0.05	1398	0.62	50	3	1.00
	0.5	3320	0.54	322	100	0.74
	1.0	3846	0.52	354	100	0.70
	1.5	4056	0.52	378	119	0.72
	2.0	4129	0.52	371	122	0.74
	3.0	4196	0.52	366	126	0.70
	4.0	4233	0.52	367	125	0.71
	10.0	4295	0.53	368	112	0.74
(b)	1.0	3156	0.55	289	39	0.77
	2.0	3153	0.53	264	34	0.79
	3.0	3140	0.52	266	34	0.82
	4.0	3156	0.53	240	35	0.89
(c)	1.0	4569	0.54	322	120	0.73
	2.0	4530	0.52	339	116	0.75
	3.0	4490	0.52	349	119	0.76
	4.0	4461	0.52	371	124	0.81
(d)	1.0	2170	0.43	176	55	0.07
	2.0	2185	0.37	193	70	0.06
	3.0	2212	0.35	188	73	0.05

TABLE I: The probabilities of occurrence of collective prolate configurations (see text for details).

at the value corresponding to the rigid rotor [1]. This means that the stable mean fields generated by random interactions with high probability correspond either to near-spherical or to well deformed shape. The situation is similar in the case of the interacting boson model [19].

We define the space-fixed quadrupole moment of the axially symmetric rotor with spin J [1] as

$$Q(J) = Q_0 \frac{3K^2 - J(J+1)}{(J+1)(2J+3)} \Rightarrow -Q_0 \frac{J}{2J+3}, \quad (2)$$

where Q_0 is the intrinsic (body-fixed) quadrupole moment, and we assume $K = 0$ for the yrast band of an even-even nucleus. Prolate intrinsic shapes, $Q_0 > 0$, correspond to squeezed shapes around the axis of collective rotation, $Q < 0$. With the standard [1] definition of the $B(E2)$ probability for the yrast band of a well deformed rotor, the Alaga ratio (1) is equal to 4.10.

In the single- j model [22], where the splitting of a j -level proceeds fan-like with approximate symmetry of oblate and prolate sides, the sign of Q will be random. Therefore we expect the crucial role of mixing of spheri-

cal orbitals. It was often suggested [26] that the spherical SM can realistically describe deformation if one uses at least two s.p. orbits with $\Delta j = 2$. This approach successfully produces collective bands, such as in ^{48}Cr , and even in the double magic ^{56}Ni [27]. The collectivity was tested not only by the $J(J+1)$ behavior, but also by large and consistent in band quadrupole moments and $B(E2)$ strengths. As a generic example, we consider a model with four neutrons and four protons in the space of two spherical orbitals, $0f_{7/2}$ and $1p_{3/2}$, of the same parity. This corresponds to the oversimplified SM description of ^{48}Cr , the nucleus with well known collective properties. Without interactions, we would have half-filled $f_{7/2}$ orbitals with zero quadrupole moment. In this space the most general rotationally invariant two-body interaction is described by 30 matrix elements, Table II below. We choose the random ensemble defined by the uniform distribution of uncorrelated matrix elements between $-V$ and $+V$, and the only parameter is the ratio $\lambda = V/\epsilon$, where ϵ is the (non-random) spacing between the two orbitals. With the statistics of 10000 realizations for each value of λ , the results are presented in Table Ia.

The case of very small $\lambda = 0.05$ can be viewed as the single- j result. The column $N(0, 2)$ shows the number of realizations with the sequence $0^+, 2^+$ of the g.s. and the first excited state. The probability of such sequences is strongly enhanced. Before applying additional requirements we can find the sign of the expectation value (2) of the quadrupole moment $Q(2^+)$. As expected, the fraction $N(Q < 0)/N(0, 2)$ of “prolate” cases, $Q < 0$, is stable near 50% (the third column). Among these states there are cases with rotational properties. The constraint that the ratio $E(4^+)/E(2^+)$ be between 3 and 3.6 (the rigid rotor would give 3.33) leaves the number of states indicated in the column $N(E4/E2)$. In the column N_{rot} we count the states where, in addition to the energy criterion, the Alaga ratio (1) is between 3.90 and 4.30, an arbitrary but restrictive choice. The last column gives the fraction of states with negative sign of Q among all “rotational” states. The predominance of prolate configurations is practically independent on the relative strength of mixing between the orbitals if this strength is sufficient for the onset of deformation. The full histogram of the distribution of the Alaga ratio is shown in Fig. 1 for two values of the interaction strength; this figure shows also the statistics without any rotational selection cuts. The prolate deformed peak is quite narrow. With the only energy criterion ($0^+, 2^+$) applied, we see also a large peak for spherical configurations with A close to zero, as well as intermediate background situations. In this large set, the prolate cases appear only in slightly more than 50% cases. We can also note that at very weak mixing, $\lambda = 0.05$, the numbers $N(0, 2)$ and especially $N(E4/E2)$ fall sharply, and the number of rotational configurations satisfying our criteria is very small. This emphasizes the importance of orbital mixing.

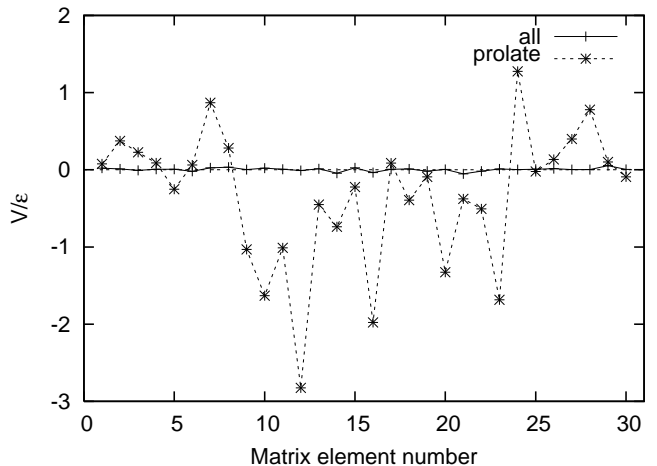


FIG. 2: The average matrix elements of the two-body interaction. The matrix element number is as in Table II.

Going from the isospin-symmetric case with $N = Z$ to asymmetric one, we consider next the system with six neutrons and four protons assuming the same set of two s.p. levels. The results are shown by Table Ib. The fraction of states with $Q < 0$ among all sequences ($0^+, 2^+$) is still close to 1/2. The total number of rotational cases is now significantly lower. At the same time, the fraction of prolate configurations is even higher than in the symmetric case. The results are essentially the same in the $N = Z$ case for the inverted level scheme when the spherical $p_{3/2}$ level is placed below the $f_{7/2}$ level, see Table Ic. Again for the very weak mixing, $\lambda = 0.01$, we do not find any rotational states; in this case all eight nucleons occupy the lowest $p_{3/2}$ level creating the closed shell. With strong level mixing, 45% of all states belong to the ($0^+, 2^+$) sequence. Clearly, the occurrence of prolate deformation is even higher than for the normal fp level sequence. This confirms the presence of the effect we mentioned in the introduction, namely the influence of the splitting of the level with higher ℓ when low- $|m|$ components steeply go down with the prolate deformation. The last case we consider here contains four protons and four neutrons in the space of two levels of opposite parity, $f_{5/2}$ and $g_{9/2}$, Table Id. Here the fraction of the sequences $0^+, 2^+$ is lower, and practically all rotational states have oblate deformation. It is clear that, due to parity conservation, direct mixing of split levels by the deformed mean field is impossible and only pairwise transfers of particles can play a role.

The main new dimension brought in by our approach is in the visualization of the entire parameter space. The mechanism of the prolate predominance is revealed as we identify the realizations of the ensemble responsible for the effect. Fig. 2 shows all 30 reduced matrix elements $\langle j_1, j_2 || V || j_3, j_4 \rangle (JT)$ allowed by angular momentum and isospin for the strong coupling limit, $\lambda = 4.0$, in case (a) of Table II. The average value of each matrix element over the whole ensemble is zero, with small fluctuations (solid

	$\langle j_1 j_2 V j_3 j_4 \rangle (JT)$	Full average	Prolate average
1	$\langle ff V ff \rangle (10)$	0.021	0.078
2	$\langle ff V ff \rangle (30)$	0.012	0.374
3	$\langle ff V ff \rangle (50)$	-0.007	0.227
4	$\langle ff V ff \rangle (70)$	0.007	0.089
5	$\langle ff V ff \rangle (01)$	0.008	-0.252
6	$\langle ff V ff \rangle (21)$	-0.020	0.062
7	$\langle ff V ff \rangle (41)$	0.026	0.869
8	$\langle ff V ff \rangle (61)$	0.034	0.282
9	$\langle ff V pf \rangle (30)$	0.004	-1.033
10	$\langle ff V pf \rangle (50)$	0.022	-1.630
11	$\langle ff V pf \rangle (21)$	0.006	-1.010
12	$\langle ff V pf \rangle (41)$	-0.010	-2.826
13	$\langle ff V pp \rangle (10)$	0.014	-0.451
14	$\langle ff V pp \rangle (30)$	-0.043	-0.739
15	$\langle ff V pp \rangle (01)$	0.025	-0.223
16	$\langle ff V pp \rangle (21)$	-0.036	-1.977
17	$\langle pf V pf \rangle (20)$	0.007	0.088
18	$\langle pf V pf \rangle (30)$	0.010	-0.393
19	$\langle pf V pf \rangle (40)$	-0.018	-0.092
20	$\langle pf V pf \rangle (50)$	0.004	-1.328
21	$\langle pf V pf \rangle (21)$	-0.052	-0.376
22	$\langle pf V pf \rangle (31)$	-0.019	-0.507
23	$\langle pf V pf \rangle (41)$	0.011	-1.685
24	$\langle pf V pf \rangle (51)$	-0.003	1.276
25	$\langle pf V pp \rangle (30)$	0.007	-0.023
26	$\langle pf V pp \rangle (21)$	0.014	0.133
27	$\langle pp V pp \rangle (10)$	0.003	0.400
28	$\langle pp V pp \rangle (30)$	0.003	0.779
29	$\langle pp V pp \rangle (01)$	0.054	0.102
30	$\langle pp V pp \rangle (21)$	0.005	-0.092

TABLE II: List of average matrix elements for the case of Table Ia and $\lambda = 4.0$.

line). The dashed line shows the average over prolate rotational samples. Table II displays the ordering of the matrix elements and their average numerical values. Although all matrix elements are enhanced compared to the level of fluctuations, one can conclude that certain matrix elements are crucial for the transition from spherical shape to predominantly prolate axial deformation. We see the exceptional role of amplitudes 9-12 describing the transfer of a single nucleon $f_{7/2} \leftrightarrow p_{3/2}$ in the interaction with another $f_{7/2}$ nucleon, regardless of its isospin. Such a process is forbidden for the orbitals of opposite parity. This agrees with the idea discussed in Ref. [12]. The monopole pairing given by amplitudes 5,15 and 29 is not effective in this transition. Contrary to that, we see a large negative amplitude of quadrupole pair transfer 16. Large quadrupole-quadrupole forces in the particle-hole channel correspond to matrix elements 20-24 in the particle-particle channel. They induce the collectivization process and formation of the proper symmetry of the mean field after mixing p - and f -orbitals.

In summary, for the first time we performed the exploration of the parameter space that serves as an arena for effective nucleon-nucleon interactions building the stable deformed mean field. We show the decisive role of the mixing between the valence spherical orbitals of the same parity split as a function of deformation. This mix-

ing, different for the two sides of the axial deformation diagram, makes the prolate deformation energetically favorable with high probability. This picture is supported by the statistical analysis of the random interaction ensemble and by singling out the responsible components of the effective interaction. The process is amplified by the presence of two kinds of nucleons. Although we have shown in detail in this Letter only cases of simple configurations, the results are quite generic for a small system. The effect is driven by the surface orbitals but it still remains to see if it indeed disappears in the macroscopic limit as predicted in Ref. [12]. The random interaction ensemble provides a new powerful tool for understanding the many-body mechanisms of collective phenomena.

Support from the NSF grant PHY-0758099 is acknowledged. V.Z. is grateful to S. Frauendorf, I. Hamamoto, B. Mottelson and A. Volya for useful discussions.

-
- [1] A. Bohr and B.R. Mottelson, *Nuclear Structure*, vol. 2 (Benjamin, New York, 1989).
- [2] B. Mottelson, *private communication*.
- [3] R.H. Lemmer, Phys. Rev. **117**, 1551 (1960).
- [4] S.G. Nilsson, Kgl. Dan. Vid. Selsk. Mat.-fys. Medd. **29**, No. 16 (1955).
- [5] B. Castel and K. Goeke, Phys. Rev. C **13**, 1765 (1976).
- [6] B. Castel, D.J. Rowe, and L. Zamick, Phys. Lett. B **236**, 121 (1990).
- [7] H. Frisk, Nucl. Phys. **A511**, 309 (1990).
- [8] M.A. Deleplanque *et al.*, Phys. Rev. C **69**, 044309 (2004).
- [9] K. Arita, A. Sugita, and K. Matsuyanagi, Czechoslovak J. Phys. **48**, 821 (1998).
- [10] I. Hamamoto, B.R. Mottelson, H. Xie, and X.Z. Zhang, Zeitschr. Phys. D **21**, 163 (1991).
- [11] J. Martin, M. Torrell, A.A. Korobkov, and J. Valles, Plant Biol. No. 5, 85 (2003).
- [12] I. Hamamoto and B.R. Mottelson, Phys. Rev. C **79**, 034317 (2009).
- [13] N. Tajima, Y.R. Shimizu, and N. Suzuki, Prog. Theor. Phys. Suppl. **146**, 628 (2002).
- [14] T.A. Brody *et al.*, Rev. Mod. Phys. **53**, 385 (1981).
- [15] V. Zelevinsky, *et al.*, B.A. Brown, N. Frazier, and M. Horoi, Phys. Rep. **276**, 85 (1996).
- [16] C.W. Johnson, G.F. Bertsch, and D.J. Dean, Phys. Rev. Lett. **80**, 2749 (1998).
- [17] M. Horoi, B.A. Brown, and V. Zelevinsky, Phys. Rev. Lett. **87**, 062501 (2001).
- [18] P. Chau Huu-Tai, A. Frank, N.A. Smirnova, and P. Van Isacker, Phys. Rev. C **66**, 061302 (2002).
- [19] R. Bijker and A. Frank, Phys. Rev. C **65**, 044316 (2002).
- [20] D. Mulhall, A. Volya, and V. Zelevinsky, Phys. Rev. Lett. **85**, 4016 (2000).
- [21] T. Papenbrock and H.A. Weidenmüller, Nucl. Phys. **A757**, 422 (2005).
- [22] V. Zelevinsky and A. Volya, Phys. Rep. **391**, 311 (2004).
- [23] Y.M. Zhao, A. Arima, and N. Yoshinaga, Phys. Rep. **400**, 1 (2004).
- [24] H.A. Weidenmüller and G.E. Mitchell, arXiv 0807.1070.
- [25] C.W. Johnson, H. Nam, Phys. Rev. C **75**, 047305 (2007).
- [26] E. Caurier *et al.*, Rev. Mod. Phys. **77**, 427 (2005).
- [27] M. Horoi *et al.*, Phys. Rev. C **73**, 061305(R) (2006).